Journal of Advanced Research in Fluid Mechanics and Thermal Sciences 110, Issue 1 (2023) 79-96

SEMARAK ILMU PUBLISHING

Journal of Advanced Research in Fluid Mechanics and Thermal Sciences

Journal homepage: https://semarakilmu.com.my/journals/index.php/fluid_mechanics_thermal_sciences/index
ISSN: 2289-7879

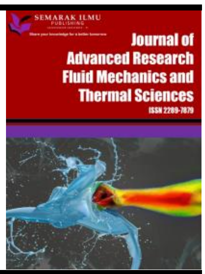

Impact of Nanoparticles Shapes on Magnetohydrodynamic Flow and Heat Transfer of Casson Hybrid Nanofluids over a Moving Inclined Plate

Mohd Rijal Ilias[1], Siti Shuhada Ishak[1], Noorehan Awang[2], Norsyasya Zahirah Mohd Zukri[1], Roselah Osman[1], Fazillah Bosli[3,*]

[1] School of Mathematical Sciences, College of Computing, Informatics and Mathematics, Universiti Teknologi MARA, 40450 Shah Alam, Selangor, Malaysia
[2] Mathematical Sciences Studies, College of Computing, Informatics and Mathematics, Universiti Teknologi MARA (UiTM) Negeri Sembilan Branch, Seremban Campus, 70300 Seremban, Negeri Sembilan, Malaysia
[3] Mathematical Sciences Studies, College of Computing, Informatics and Mathematics, Universiti Teknologi MARA (UiTM) Kedah Branch, Sungai Petani Campus, 08400 Merbok, Kedah Darul Aman, Malaysia

ARTICLE INFO

Article history:
Received 11 June 2023
Received in revised form 5 September 2023
Accepted 18 September 2023
Available online 6 October 2023

Keywords:
Magnetohydrodynamics (MHD); Convective Boundary Conditions; Casson Hybrid Nanofluids; Moving Inclined Plate; Nanoparticles Shape

ABSTRACT

This study investigated the impact of different nanoparticles shape on magnetohydrodynamic of Casson hybrid nanofluids flow and heat transfer over a moving inclined plate with convective boundary conditions. The study infused water with silver (Ag) and Titanium Oxide (TiO_2) to analysed the velocity and temperature profiles as well as skin friction and Nusselt number. The numerically method solved by by applying the implicit finite difference, Keller Box method based on similarity transformation techniques that used to convert the partial differential equations of Casson hybrid nanofluids to an ordinary differential equation. The results showed that platelet shaped nanoparticles had the highest velocity and temperature profiles, while a parameter of aligned angle of magnetic field, α, interaction of magnetic field, M, mixed convection parameters, λ_T, inclined angle parameters, γ, Casson parameters, β_c, and Biot numbers, Bi_x is increased, the velocity is increased and temperature is decreased. Conversely, as the volume fraction of nanoparticles, (ϕ_1, ϕ_2) is increased, the velocity is decreased and temperature is increased. For moving inclined plate, the highest skin friction is moving against the flow while moving along the flow plate has the highest Nusselt number. The findings of the study can be useful in designing and optimizing various industrial applications that involve the transport of Casson hybrid nanofluids.

1. Introduction

Heat transfer fluids are used in a variety of industrial applications where the transfer of heat is necessary for efficient operation. Fluid is commonly employed as heat transporters in transportation systems and industrial operations, such as for heating and cooling. In most applications, heat transfer fluids are utilized as cooling fluids, such as water, oil, ethylene glycol etc. The heat transfer of working fluids is improved using various techniques, one of which is to suspend nanoparticles to the working

* *Corresponding author.*
E-mail address: fazillah@uitm.edu.my

https://doi.org/10.37934/arfmts.110.1.7996

fluid. Nanofluids are a type of fluid that contains suspended nanoparticles with sizes typically in the range of 1 to 100 nanometers. Choi and Eastman [1] was the first study on the heat transfer in nanofluids by adding nanoscale particles to a base fluid and the nanofluids have a higher thermal conductivity and have a greater effect on heat transfer. Consequently, many researchers have numerically and experimentally investigated the behavior and properties of nanofluids from various aspects. Tiwari and Das [2] is one of the examples who proposed mathematical models for nanofluids that study the behavior of nanofluids considering the effects of the solid volume fractions of nanoparticles.

On the other hands, a relatively new type of nanofluids that can be made by suspending two or more types of nanoparticles in a base fluid to improve a higher thermal conductivity and have a greater effect on heat transfer have been widely used [3]. Hybrid nanofluids are a type of nanotechnology that is rapidly expanding due to their potential applications in material science and engineering. The thermal properties of hybrid nanofluids can be tuned by varying the size, shape, and concentration of the nanoparticles and microparticles. The thermal performance of hybrid nanofluids is investigated through experiments that measure their thermal conductivity, viscosity, and heat transfer coefficient by Sidik *et al.,* [4]. The results show that the thermal performance of hybrid nanofluids is strongly influenced by the nanoparticle type, size, concentration, and preparation method and potential for various industrial applications that require high heat transfer rates, such as cooling systems and heat exchangers. Manjunatha *et al.,* [5] found a significant improvement in thermal conductivity by adding metallic nanoparticles as a hybrid nanofluids to the base fluids. Akbar *et al.,* [6] theoretically investigated a heat performance by considering an alumina and titania suspended in water. It found that heat transfer enhancement increases by increasing of hybrid nanofluids volume concentration and volume flow rate. Most of the researchers attracted towards the hybrid nanofluids in their research work on theoretical research on the different situation [7-12].

Casson hybrid nanofluids are a type of hybrid nanofluid that contains nanoparticles dispersed in a Casson fluid. A Casson fluid is a type of non-Newtonian fluid that exhibits a yield stress and a shear thinning behaviour. Rawi *et al.,* [13] investigated an unsteady mixed convection flow of a Casson fluid in the presence of nanoparticles and founds that the skin friction coefficient and Nusselt number increase with an increase in nanoparticle concentration, while the velocity and temperature profiles decrease. By considering the magnetohydrodynamic (MHD) to facilitate the formation of a stable thermal boundary layer around the heated surface, leading to improved heat transfer in this study. Several studies have revealed that with the presence of MHD effect give a significant impact. Studied by Mohamad *et al.,* [14] and Bosli *et al.,* [15] have not dealt with Casson hybrid nanofluids but in Casson nanofluids with the presence of a magnetic field. Mohamad *et al.,* [14] found that an increase in Casson nanofluids and magnetic have decrease the Nusselt number whereas Bosli *et al.,* [15] founds that the Casson parameter have increase the velocity profile and heat transfer while the temperature and skin friction has decrease. The studied of a Casson hybrid nanofluids with MHD effect by Krishna *et al.,* [16] reveals that the magnetic field and Casson parameters have a significant impact on the flow behaviour of the nanofluids. Also, an increase in volume fraction of nanoparticles causes an increment through the temperature profiles, whereas the temperature of Casson hybrid Ag-TiO_2/WEG nanofluids is relatively greater than that of Casson Ag-WEG nanofluids. Aman *et al.,* [17] investigated the presence of MHD on the unsteady flow and founds that an increases values Casson parameter, the velocity is increase while velocity is decrease when magnetic parameter is increases. There have been several investigations into the MHD effect in different problems and found that MHD effect have an important impact on the boundary layer flow [18-29].

Nanoparticle shape is important in heat transfer because it affects the thermal properties of the nanoparticle and the thermal conductivity of the hybrid nanofluids. The thermal conductivity of a nanofluid is influenced by several factors, including the shape and size of the nanoparticles. The previous study by Rashid and Adnan [30] investigated the effects of nanoparticles shape with the presence of magnetic field. They used five different shapes of nanoparticles which are column, sphere, hexahedron, tetrahedron and lamina and found that lamina shapes nanoparticles have greater heat transfer and temperature other than shapes of nanoparticle. Anwar *et al.,* [31] investigated in the thermal performance of NaAlg-MoS_2-Co hybrid nanofluid under different shape factors. The result founds that the thermal conductivity of the nanofluid increases with the increase in volume fraction and temperature while blade shape has highest of the heat transfer. The MHD and convective heat transfer of nanofluids synthesized by three different shaped (brick, platelet, and cylinder) silver (Ag) nanoparticles in water was analyzed by Akbar and Butt [32]. The computations showed that pressure increases with enhancing the buoyancy force and nanoparticle fraction however it reduces with increasing the magnetic field. Also, reveals that pressure enhancement is a maximum for the platelet nanoparticle case compared with the brick and cylinder nanoparticle cases. Jamshed *et al.,* [33] discussed the analysis of entropy generation a hybrid nano liquid composed of $MgZn_6Zr$-Cu and ethylene oxide (EO) considering the nanoparticle shape. The result found that the presence of nanoparticles in the hybrid nano liquid reduces the entropy generation rate and lamina-shaped layer's components have the highest thermal conductivity, while sphere-shaped nanoparticles have the lowest. The effect of nanoparticles shapes on MHD Casson hybrid nanofluids flows over a moving vertical plate was studied by Zukri *et al.,* [34] found that the nanoparticles shape of platelets has the highest velocity and temperature profiles, followed by cylindrical, bricks, and spherical shape while the magnetic field parameter and Casson hybrid nanofluids indicated the velocity increases while the temperature decreases. The shape of the nanoparticles can affect their sedimentation and agglomeration behavior, which can impact the stability and effectiveness of the nanofluid. Therefore, the shape of nanoparticles is a crucial factor that should be considered when designing hybrid nanofluids for specific applications, as it can affect their thermal, rheological, and stability properties.

Studies are done in the area of Casson hybrid nanofluids in various situation while there is a lack for situation of moving plate. Thus, the aim of the present research work is to study the effect of aligned MHD and nanoparticle shape of a Casson hybrid nanofluids past a moving inclined. It is seeming that the influence of both nanoparticle shape effect and hybrid nanofluids plays a crucial role in enhancing thermal conductivity of fluid. The model of Tiwari and Das [2] is employed in this study to deal with governing equations by including hybrid nanoparticles, such as Silver (Ag) and Titanium oxide (TiO_2), with water as the base fluid.

2. Mathematical Formulation

Consider a mixed convection flow of an incompressible Casson hybrid nanofluids over a moving inclined plate parallel to the direction of the generating body force, as shown in Figure 1. The rheological equation for an isotropic and incompressible Casson fluid, reported by Casson [35], is

$$\tau_{ij} = \begin{cases} \left(\mu_B + p_y/\sqrt{2\pi}\right)2e_{ij} & , \quad \pi > \pi_c \\ \left(\mu_B + p_y/\sqrt{2\pi_c}\right)2e_{ij} & , \quad \pi < \pi_c \end{cases}$$

where μ_B is plastic dynamic viscosity of non-Newtonian fluid, p_y is yield stress, π_c is critical value of this product based on the non-Newtonian model and π is the product of the component of deformation rate with itself, namely $\pi = e_{ij}e_{ij}$, e_{ij} is the $(i,j)^{th}$ component of deformation rate. The plate is moving with constant velocity $U_w = \varepsilon U_\infty$, where U_w is the plate velocity, ε is the plate velocity parameter and x and y are the coordinates system measured along the moving plate. An aligned magnetic field with an acute angle, α as shown in Figure 1 is applied to the flow. It is recognized as the origin function as expressed by $B_x = \frac{B_0}{\sqrt{x}}$ with $B_0 \neq 0$.

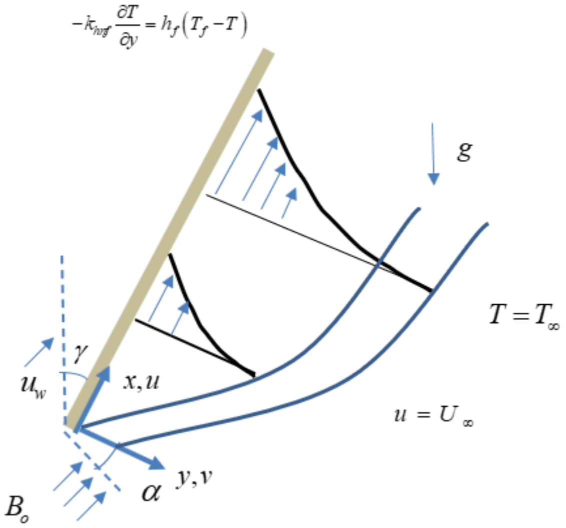

Fig. 1. Geometry Flow of Moving Inclined Plate

The mathematical model is considered under the following assumptions and conditions:

(i) Two-Dimensional laminar steady flow;
(ii) Boundary layer approximation;
(iii) Non-Newtonian Casson hybrid nanofluids;
(iv) Aligned Magnetohydrodynamics (MHD);
(v) Nanoparticles shape factor;
(vi) Convective boundary conditions;

Under the presumptions outlined above, the governing boundary layer equations of the hybrid nanofluid by employing the usual approximations of the boundary layer for the continuity, momentum and energy equations can be written as [15];

$$\frac{\partial u}{\partial x} + \frac{\partial v}{\partial y} = 0 \tag{1}$$

$$u\frac{\partial u}{\partial x} + v\frac{\partial u}{\partial y} = \frac{\mu_{hnf}}{\rho_{hnf}}\left(1 + \frac{1}{\beta_c}\right)\frac{\partial^2 u}{\partial y^2} + \frac{(\rho\beta)_{hnf}}{\rho_{hnf}} g \cos\gamma\,(T - T_\infty) - \frac{\sigma B^2(x)}{\rho_{hnf}} sin^2\alpha(u - U_\infty) \tag{2}$$

$$u\frac{\partial T}{\partial x} + v\frac{\partial T}{\partial y} = \alpha_{hnf}\frac{\partial^2 T}{\partial y^2} \tag{3}$$

While the boundary conditions used in this study are as follows:

$$\begin{aligned} &u = u_w = \varepsilon U_\infty, \quad v = 0, \quad -k_{hnf}\frac{\partial T}{\partial y} = h_f\left(T_f - T\right), \quad on\ y = 0 \\ &u \to U_\infty, \quad T \to T_\infty \quad as\ y \to \infty \end{aligned} \tag{4}$$

where u is the fluid velocity and v is the normal velocity components along the x-axis and y-axis. While, α is the angle of magnetic field, γ is the angle of inclined plate, T is the temperature of the fluids, T_f is the nanofluids temperature, T_∞ is the free stream temperature, g is the gravity acceleration, U_∞ is the free stream velocity, ρ_{hnf} is the effective density, σ is the electrical conductivity, $(\rho\beta)_{hnf}$ is the thermal expansion coefficient, μ_{hnf} is the effective dynamic viscosity, α_{hnf} is the thermal diffusivity of the fluid, $(\rho C_p)_{hnf}$ is the heat capacity of the fluid, k_{hnf} is the thermal conductivity of the hybrid nanofluids, M is the magnetic parameter, h_f is the heat transfer coefficient of fluid, and β_c is the Casson hybrid nanofluids parameter. Table 1 is representing the shape factor (m) and its numerical shape factor for different kind of shapes. Shape factor, $m = \frac{3}{Z}$ should be noted, where Z is the sphericity. Sphericity is the ratio of the surface area of the sphere as well as the surface area of the real particles with equal volumes. Sphericity of sphere, platelet, cylinder, and brick are 1.000, 0.526, 0.625, and 0.811, respectively. The shape factor of the particle is 3 which is $m = 3$ when The Hamilton-Crosser model becomes a Maxwell-Garnett model. The shape factor m is obtained from [1,52,54]. The velocity and temperature profile are important in solving this study but shape factor also played a role in determining what and which shapes gives a better result. Different shape has a different numerical shape factor. This shape factor determines whether the shape is suitable enough with the nanoparticles. The nanoparticles shape factors, m shown in Table 1 and Table 2 display the thermophysical relations in nanoparticles shape of hybrid nanofluids [3,15].

Table 1
The Nanoparticles Shape Factors (m) [16,31,32]

Nanoparticles Shape	Shapes	Shape Factor (m)	Sphericity (Z)
Spherical		3.0	1.000
Platelets		5.7	0.526
Cylindrical		4.8	0.625
Bricks		3.7	0.811

Table 2
Thermophysical Relation in Nanoparticles Shape of Hybrid Nanofluids [3,15]

Properties	Hybrid Nanofluids	
Density	$\rho_{hnf} = (1-\phi_2)\left[(1-\phi_1)\rho_f + \phi_1\rho_{s1}\right] + \phi_2\rho_{s2}$	(7)
Heat Capacity	$(\rho C_p)_{hnf} = (1-\phi_2)\left[(1-\phi_1)(\rho C_p)_f + \phi_1(\rho C_p)_{s1}\right] + \phi_2(\rho C_p)_{s2}$	(8)
Viscosity	$\mu_{hnf} = \dfrac{\mu_f}{(1-\phi_1)^{2.5}(1-\phi_2)^{2.5}}$	(9)
Thermal Conductivity	$\dfrac{k_{hnf}}{k_{bf}} = \dfrac{k_{s2} + (m-1)k_{bf} - (m-1)\phi_2(k_{bf} - k_{s2})}{k_{s2} + (m-1)k_{bf} - \phi_2(k_{bf} - k_{s2})}$	(10)
	$\dfrac{k_{bf}}{k_f} = \dfrac{k_{s1} + (m-1)k_f - (m-1)\phi_1(k_f - k_{s1})}{k_{s1} + (m-1)k_f - \phi_1(k_f - k_{s1})}$	(11)
	$k_{bf} = \dfrac{k_{s1} + (m-1)k_f - (m-1)\phi_1(k_f - k_{s1})}{k_{s1} + (m-1)k_f - \phi_1(k_f - k_{s1})} \times k_f$	
	$\dfrac{k_{hnf}}{k_f} = \dfrac{k_{hnf}}{k_{bf}} \times \dfrac{k_{bf}}{k_f} = \dfrac{k_{s2} + (m-1)k_{bf} - (m-1)\phi_2(k_{bf} - k_{s2})}{k_{s2} + (m-1)k_{bf} - \phi_2(k_{bf} - k_{s2})} \times \dfrac{k_{s1} + (m-1)k_f - (m-1)\phi_1(k_f - k_{s1})}{k_{s1} + (m-1)k_f - \phi_1(k_f - k_{s1})}$	
	where	
	$\dfrac{k_{bf}}{k_f} = \dfrac{k_{s1} + (m-1)k_f - (m-1)\phi_1(k_f - k_{s1})}{k_{s1} + (m-1)k_f - \phi_1(k_f - k_{s1})}$	
Thermal Expansion Coefficient	$\beta_{hnf} = (1-\phi_2)\left[(1-\phi_1)\beta_f + \phi_1\beta_{s1}\right] + \phi_2\beta_{s2}$	(12)
	$(\rho\beta)_{hnf} = (1-\phi_2)\left[(1-\phi_1)(\rho\beta)_f + \phi_1(\rho\beta)_{s1}\right] + \phi_2(\rho\beta)_{s2}$	(13)
Thermal Diffusivity	$\alpha_{hnf} = \dfrac{k_{hnf}}{(\rho C_p)_{hnf}}$	(14)

Table 3 shows the thermophysical properties of base fluid which is water and nanoparticles taken from Krishna *et al.,* [16]. The nanoparticles that will be used in this current research are Ag (Silver) and TiO_2 (Titanium Oxide).

Table 3
Thermophysical Properties of Base Fluid and Hybrid Nanofluids [16]

Properties	Base Fluid (Water)	Ag (Silver)	TiO_2 (Titanium Oxide)
$\rho(kg/m^3)$	997.1	10500	4250
$C_p(J/kgK)$	4179	235	686.2
$k(W/mk)$	0.613	429	8.9538
$\beta \times 10^{-5}$	21	1.89	0.9
Pr	6.20		

The continuity Eq. (1) is satisfied by introducing stream function $\psi(x, y)$ as shown below,

$$u = \frac{\partial\psi}{\partial y}, v = -\frac{\partial\psi}{\partial x} \quad (15)$$

The following similarity variables are introduced to solve the governing Eq. (1) to Eq. (3),

$$\eta = \frac{y}{x}(Re_x)^{\frac{1}{2}}, \qquad \psi = \upsilon_f \sqrt{Re_x} f(\eta), \qquad \theta = \frac{T - T_\infty}{T_f - T_\infty}, \tag{16}$$

where η is the similarity variable, $Re_x = \frac{U_\infty x}{v_f}$ refers to Reynolds number, $\upsilon_f = \frac{\mu_f}{\rho_f}$ is kinematic viscosity, $f(\eta)$ and $\theta(\eta)$ indicate the non-dimensional stream function and temperature, respectively.

By substituting Table 1, (15), and (16) into (2) and (3), the following nonlinear systems of ordinary differential equations are obtained:

$$\left(1 + \frac{1}{\beta_c}\right) f'''(\eta) + \frac{A_1 A_2}{2} f(\eta) f''(\eta) + A_1 A_3 \lambda_T \cos\gamma\, \theta(\eta) + A_1 M sin^2\alpha \left(1 - f'(\eta)\right) = 0 \tag{17}$$

$$A_4 \theta''^{(\eta)} + \frac{Pr}{2} A_5 f(\eta) \theta'(\eta) = 0 \tag{18}$$

By respecting to (4), the boundary conditions obtained are as follows:

$$\begin{aligned} &f(0) = 0, \ \ f'(0) = \varepsilon, \ \ \theta'(0) = -Bi_x\left(1 - \theta(0)\right) \quad \text{at} \quad y = 0 \\ &f'(\eta) = 1, \ \ \theta(\eta) = 0 \quad \text{as} \quad y \to \infty \end{aligned} \tag{19}$$

The discussions of numerical results are based on the skin friction coefficient, C_f at the surface of the plate and local Nusselt number, Nu_x which are defined as:

$$C_f = \frac{\tau_w}{\rho_f {U_\infty}^2}, \quad Nu_x = \frac{x q_w}{k_f (T_f - T_\infty)} \tag{20}$$

where ρ_f is the density of nanofluids, τ_w is the shear stress or wall skin friction, q_w is the convective boundary condition and k_f is the thermal conductivity of the nanofluids.

$$\tau_w = \mu_{hnf}\left(1 + \frac{1}{\beta_c}\right)\left(\frac{\partial u}{\partial y}\right)_{y=0}, \quad q_w = -k_{hnf}\left(\frac{\partial T}{\partial y}\right)_{y=0} \tag{21}$$

By substituting (16) and (21) into (20), the solutions obtained are as follows:

$$\frac{C_f}{(Re_x)^{\frac{1}{2}}} = \left(1 + \frac{1}{\beta_c}\right)\frac{1}{A_1} f''(0), \qquad \frac{Nu_x}{(Re_x)^{\frac{1}{2}}} = -A_4 \theta'(0) \tag{22}$$

where,

$$A_1 = (1 - \phi_1)^{2.5}(1 - \phi_2)^{2.5}, \quad A_2 = (1 - \phi_2)\left\{(1 - \phi_1) + \phi_1 \frac{\rho_{s1}}{\rho_f}\right\} + \phi_2 \frac{\rho_{s2}}{\rho_f},$$

$$A_3 = (1 - \phi_2)\left\{(1 - \phi_1) + \phi_1 \frac{(\rho\beta)_{s1}}{(\rho\beta)_f}\right\} + \phi_2 \frac{(\rho\beta)_{s2}}{(\rho\beta)_f}, \qquad A_4 = \frac{k_{hnf}}{k_f}$$

$$A_5 = (1-\phi_2)\left\{(1-\phi_1)+\phi_1\frac{(\rho C_p)_{s1}}{(\rho C_p)_f}\right\}+\phi_2\frac{(\rho C_p)_{s2}}{(\rho C_p)_f},$$

$$M=\frac{\sigma {B_0}^2}{\rho_f U_\infty},\qquad \lambda_T=\frac{g(\beta)_f(T_w-T_\infty)x}{{U_\infty}^2},\qquad Pr=\frac{\mu_f(C_p)_f}{k_f},\qquad Bi_x=\frac{h_f}{k_{hnf}}\left(\frac{\upsilon_f x}{U_\infty}\right)^{\frac{1}{2}}$$

3. Numerical Solution

Eq. (17) and Eq. (18) subject to the boundary conditions (19) are solved numerically using Keller-box method as described in the books by Na and Hansen [36] and Cebeci and Bradshaw [37]. The solution is obtained in the following four steps

(i) Reduce Eq. (17) and Eq. (18) to first-order system.
(ii) Write the difference equations using central differences.
(iii) Linearize the resulting algebraic equations by Newton’s method and write them in the matrix-vector form.
(iv) Solve the linear system by the block tridiagonal elimination technique.

4. Validation

Validation of the numerical method was measured by comparing the results of $\theta(0)$ for different values of Biot Number from the current approach with the outcomes of the previous study Bataller [38], Aziz [39], Ishak *et al.,* [40] and Ramesh *et al.,* [41]. Table 4 summarizes the coherence of result of the previous study with the current result. The present findings are reported to be in fair agreement, which confirms the precision of the numerical results obtained.

Table 4
Comparison Results of $\theta(0)$ for Different Values of Biot Number (Bi_x) when $M=0$, $Pr=0.72$, and $\lambda_T=0{,}0.5$

Bi_x	$M=0$, $Pr=0.72$, and $\lambda_T=0$					$M=0$, $Pr=0.72$, and $\lambda_T=0.5$	
	Bataller [38]	Aziz [39]	Ishak *et al.,* [40]	Ramesh *et al.,* [41]	Present	Ramesh *et al.,* [41]	Present
0.05	0.1446	0.1447	0.1446	0.1446	0.144660	0.1388	0.138810
0.1	-	0.2528	0.2527	0.2527	0.252756	0.2386	0.238622
0.2	0.4035	0.4035	0.4035	0.4035	0.403520	0.3774	0.377434
0.4	-	0.5750	0.5750	0.5750	0.575012	0.5398	0.539854
0.6	0.6699	0.6699	0.6699	0.6699	0.669914	0.6337	0.633763
0.8	-	0.7302	0.7301	0.7301	0.730168	0.6954	0.695454
1.0	0.7718	0.7718	0.7718	0.7718	0.771821	0.7392	0.739209
5	-	0.9441	0.9441	0.9441	0.944173	0.9323	0.932320
10	0.9712	0.9713	0.9712	0.9712	0.971285	0.9648	0.964825

5. Result and Discussion

The results for this study to examined the influence of the aligned angle of magnetic field, α, interaction of magnetic field, M, volume fraction of nanoparticles, (ϕ_1,ϕ_2), mixed convection parameters, λ_T, inclined angle parameters, γ, Casson parameters, β_c, and Biot numbers, Bi_x on velocity and temperature profiles as well as skin friction and Nusselt number of Casson hybrid nanofluids over a moving inclined plate. The Prandtl number taken is 6.2 and fit the nondimensional values as follows for numerical computation, $\alpha = 90°, M = 1, \phi_1 = 0.1, \phi_2 = 0.1, \gamma = 45°, \lambda_T = 0.5, \beta_c = 2$ and $Bi_x = 0.1$, unless stated otherwise. In this study, m denotes the shape factor which stated in Table 1. Figure 2 to Figure 8 shows the velocity and temperature profiles for spherical shape change with different values of $\alpha, M, \phi_1, \phi_2, \gamma, \lambda_T, \beta_c$ and Bi_x, while the numerical value of skin friction coefficient and Nusselt number for nanoparticles shape are shown in Table 5.

Figure 2(a) and Figure 2(b) show the effects of different values of the inclined angle of a magnetic field, α on the velocity and temperature profile for all conditions of the inclined plate for spherical shape. It was observed that for every condition of inclined plate, an increase in α results in the increase of the velocity profiles but a decrease in the momentum boundary layer thickness. This is due increase in applied magnetic field when the α increases cause the Casson hybrid nanofluid to be pushed towards the plate. When $\alpha = 0$ it indicates that there is no magnetic field and because of the changes in the aligned field position of the magnetic field, it attracts the nanoparticles. For all the conditions of the inclined plate, when α increases, the velocity profiles increase while the temperature profiles decrease. The thermal boundary layer thickness also decreases. As shown in Table 5, the skin friction coefficient and Nusselt number increases, as α increases. The inclined plate that has the highest result for skin friction coefficient is the inclined plate that is moving against the plate, which is 2.067450, while the inclined plate that is moving together with the plate has a Nusselt number of 0.145788.

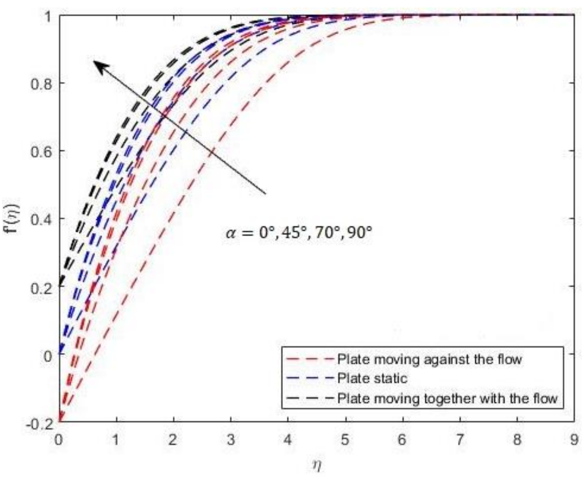

(a)

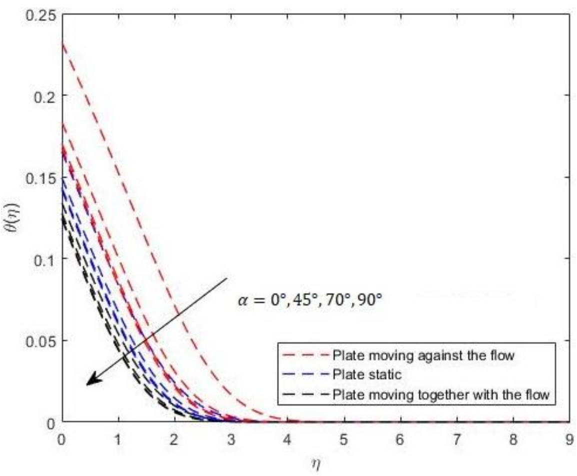

(b)

Fig. 2. Effects of α on (a) velocity profiles and (b) temperature profiles over moving inclined plate

Figure 3(a) and Figure 3(b) demonstrates the effect of different values of magnetic field, M on velocity and temperature profiles for all conditions of inclined plate for spherical shape. It is observed that when there is an increase in M, the velocity profiles increase but decline in momentum boundary layer for all conditions of inclined plate. When $M = 0$, this indicates that there is no magnetic force. It is means by when magnetic field value increase, it pushes the fluid towards the plate and thus, the momentum boundary layer decreases. An increase in M leads to an increase in Lorentz force and hence, producing more resistance to the transport phenomena. The temperature profile of all nanoparticles shape and the thermal boundary layer decrease when M increases. For the skin friction and Nusselt number, the value is increasing as M increases as shown in Table 5. The inclined plate that has highest result for skin friction coefficient is the inclined plate that is moving against the plate, which is 3.400326, while for Nusselt number is the inclined plate that is moving together with the plate with 0.147023.

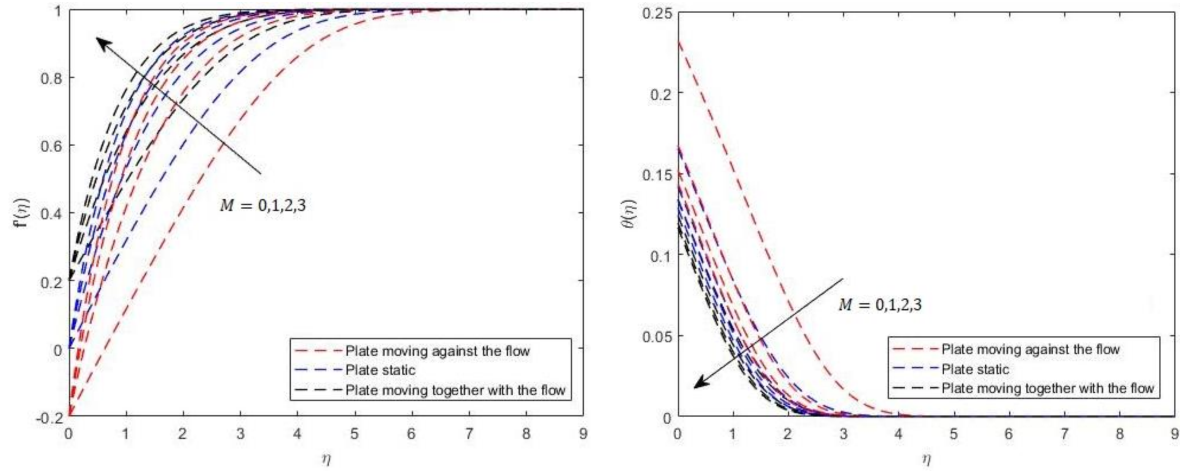

(a) (b)

Fig. 3. Effects of M on (a) velocity profiles and (b) temperature profiles over moving inclined plate

Figure 4(a) and (b) demonstrate the effect of different values of inclined angle of nanoparticle, γ, on velocity and temperature profile for all condition of inclined plate for spherical shape. The increment in γ makes the velocity profile for all inclined plate decrease and the momentum boundary layer thickness increase. For $\gamma = 90°$, the plate is horizontal and for $\gamma = 0°$, the plate assumes a vertical position. As discussed in Chapter 4, the gravitational effect is minimum for $\gamma = 90°$ and maximum for $\gamma = 0°$. As shown in Table 5, the skin friction coefficient and Nusselt number decrease as γ increases. It is noticed that inclined plate that is against the flow has the highest skin friction coefficient while for the Nusselt number, inclined plate that is along together with the flow has the highest Nusselt number.

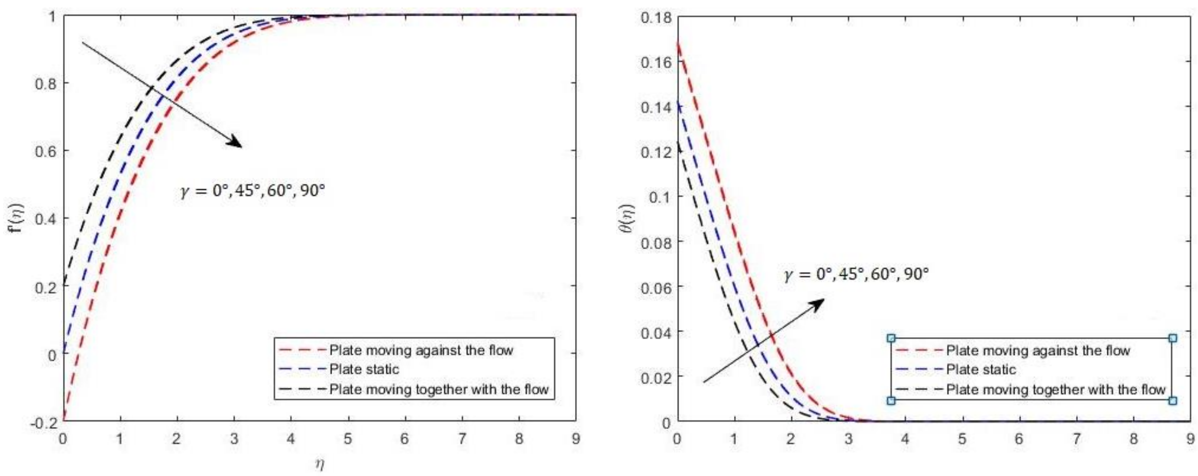

(a) (b)

Fig. 4. Effects of γ on (a) velocity profiles and (b) temperature profiles over moving inclined plate

Figure 5(a) and (b) demonstrate the effect of different values volume fraction of nanoparticle, (ϕ_1, ϕ_2), on velocity and temperature profile for all condition of inclined plate. The increment in (ϕ_1, ϕ_2)makes the velocity profile for all inclined plates decrease but increase in the momentum boundary layer thickness. This accompanies with the enhancement of viscosity that tends the velocity to fall. Then, the temperature increases when (ϕ_1, ϕ_2) increases for all condition of inclined plate. Besides that, the thermal boundary layer thickness also increases with the increase in (ϕ_1, ϕ_2). As shown in Table 5, the skin friction coefficient and Nusselt number increase as (ϕ_1, ϕ_2) increases. It is noticed that inclined plate that is against the flow has the highest skin friction coefficient while for the Nusselt number, inclined plate that is along together with the flow has the highest Nusselt number.

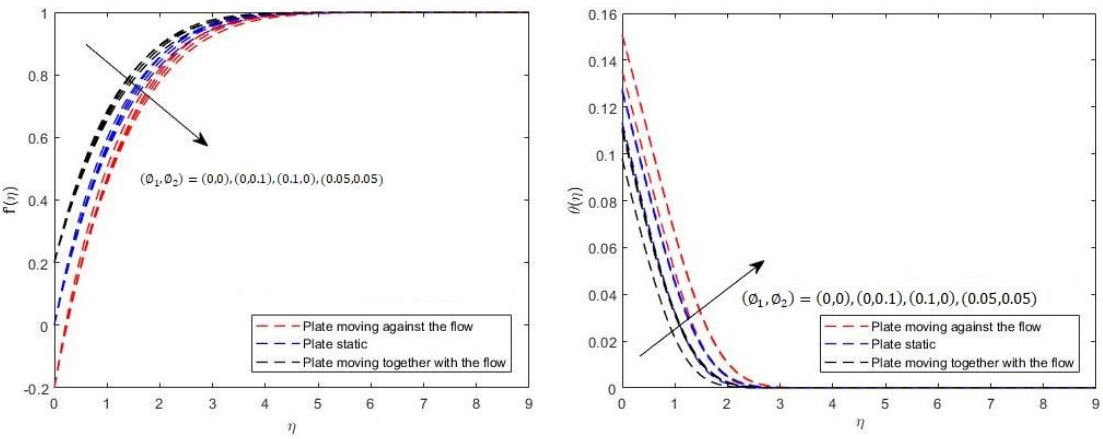

(a) (b)

Fig. 5. Effects of (ϕ_1, ϕ_2) on (a) velocity profiles and (b) temperature profiles over moving inclined plate

Figure 6(a) and (b) demonstrate the effect of different values of mixed convection parameter, λ_T, on velocity and temperature profile for all condition of inclined plate. It can be observed that when there is increment in λ_T, the temperature profiles and the thermal boundary layer will decrease for all conditions of inclined plate. As shown in Table 5, the skin friction coefficient and Nusselt number increase as λ_T increases. It is noticed that inclined plate that is against the flow has the highest skin friction coefficient while for the Nusselt number, inclined plate that is along together with the flow has the highest Nusselt number.

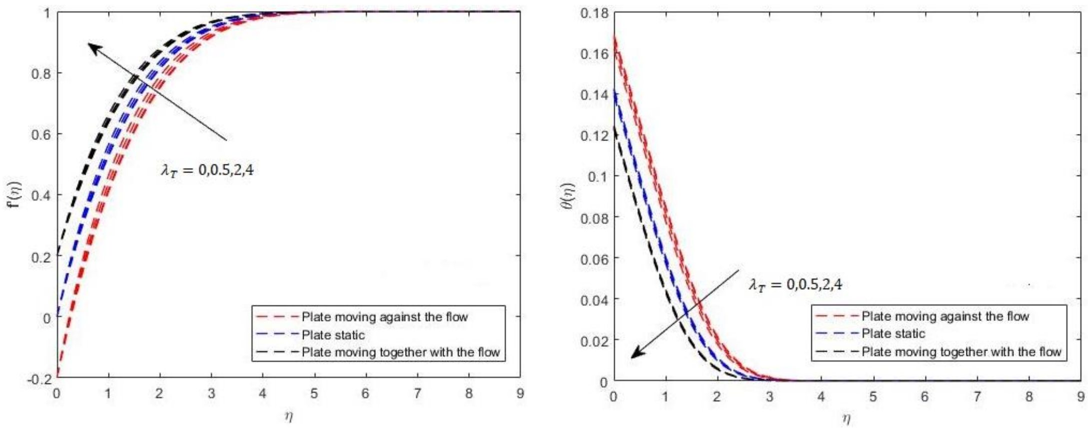

(a) (b)

Fig. 6. Effects of λ_T on (a) velocity profiles and (b) temperature profiles over moving inclined plate

Figure 7(a) demonstrates the influence of the Casson hybrid nanofluids parameter, β_c on the nanofluids velocity. The nanofluids velocity increases when β_c increases, while the thickness of boundary layer decreases. It can be explained by when there is increment in the value of β_c, the momentum equation tends to the momentum equation of a Newtonian fluid. Therefore, nanofluids velocity increases as the effective viscous drag force decreases with the increases in β_c. This is explained the reason why the nanofluids velocity reaches the free stream velocity earlier for a greater value of β_c. Figure 7(b) presents the effect of β_c on temperature profiles for all conditions of inclined plate. It is noticeable that fluid temperature decreases with the increment of β_c for all inclined plate's conditions. It is because when β_c increases, it is implying a reduction in yield stress, and therefore, the thickness of the thermal boundary layer reduces. The magnitude of skin friction coefficient is decreases as β_c increases, while Nusselt number is increase as β_c increases for all conditions of inclined plate. As noticed in Table 5, the inclined plate that is against the flow has the highest skin friction coefficient while for the Nusselt number, inclined plate that is along together with the flow has the highest Nusselt number.

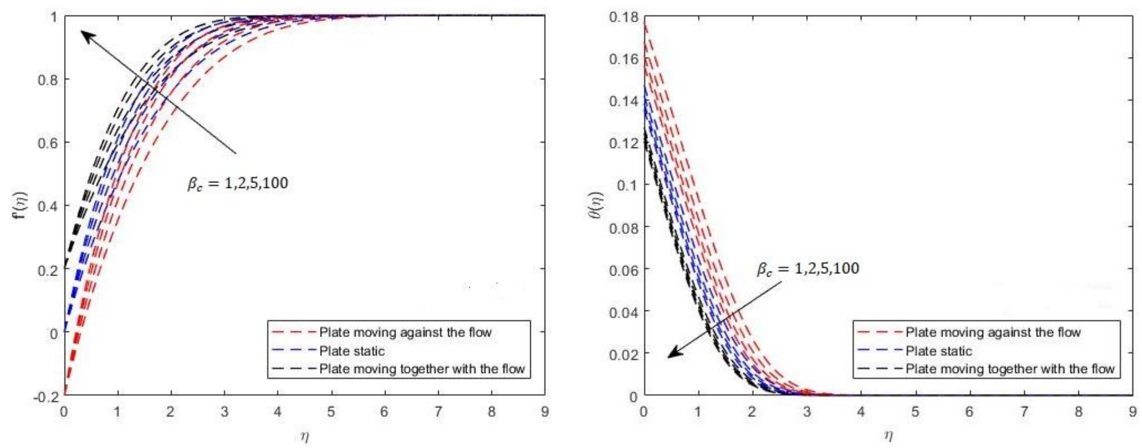

(a) (b)

Fig. 7. Effects of β_c on (a) velocity profiles and (b) temperature profiles over moving inclined

Based on Figure 8(a), demonstrate the effect of different values of Biot number, Bi_x, on velocity profile for all conditions of inclined plate. The figure shows that when there is an increase in Bi_x, the velocity profiles increases while the momentum boundary layer decreases for all conditions of inclined plate. When $Bi_x = 0$, there is no convective heat transfer and the velocity would also be low whereas when Bi_x increases, the buoyancy force becomes stronger as a result of the increase in strength of convective process of the plate. Based on Figure 8(b) demonstrates that as Bi_x increases, the temperature profile and the thermal boundary layer also increases. This is because, with an increase in Bi_x, the thermal resistance of the plate decreases and the convective heat transfer of the plate increases.

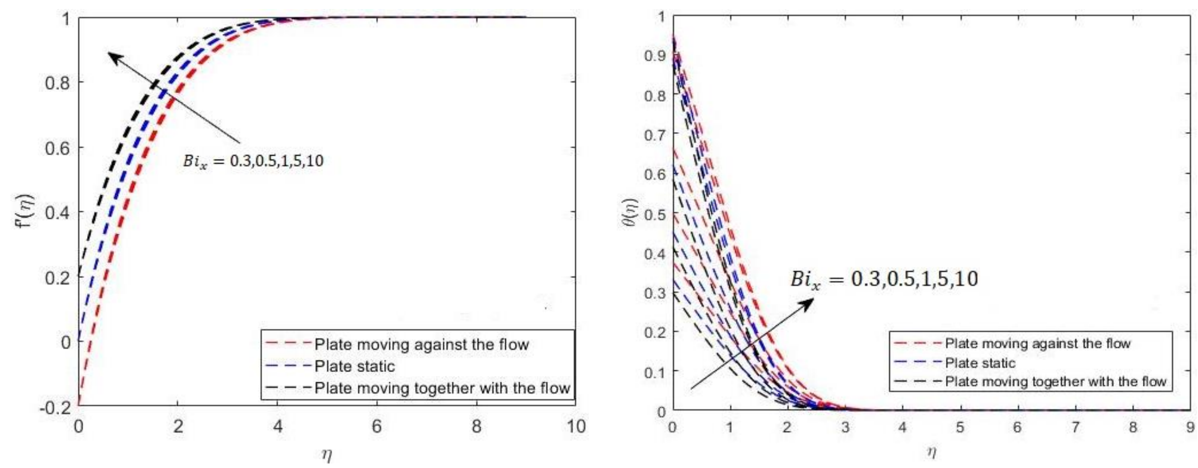

(a) (b)

Fig. 8. Effects of Bi_x on (a) velocity profiles and (b) temperature profiles over moving inclined

Table 5 shows the Skin friction and Nusselt Number of moving inclined plate for spherical shape. Meanwhile, Table 6 and Table 7 below shows the variation in skin friction coefficient and Nusselt number at different dimensionless parameters for nanoparticles shapes. The information in the following tables is derived from the static inclined plate condition.

Table 5
Variation of Skin Friction Coefficient and Nusselt Number at Different Dimensionless Parameters of Moving Inclined Plate for Spherical Shape

α	M	γ	ϕ_1	ϕ_2	λ_T	β_c	Bi_x	Spherical					
								Skin Friction			Nusselt Number		
								Against the flow $\varepsilon = -0.2$	Static $\varepsilon = 0$	Follow the flow $\varepsilon = 0.2$	Against the flow $\varepsilon = -0.2$	Static $\varepsilon = 0$	Follow the flow $\varepsilon = 0.2$
0°								0.829973	0.836165	0.772606	0.127807	0.138897	0.144103
45°	1	45°	0.1	0.1	0.5	2	0.1	1.570781	1.385998	1.170556	0.135888	0.141563	0.145170
70°								1.962237	1.696291	1.406778	0.138094	0.142584	0.145665
90°								2.067450	1.780738	1.471817	0.138573	0.142824	0.145788
	0							0.829973	0.836165	0.772606	0.127807	0.138897	0.144103
90°	1	45°	0.1	0.1	0.5	2	0.1	2.067450	1.780738	1.471817	0.138573	0.142824	0.145788
	2							2.812971	2.386281	1.943701	0.141127	0.144209	0.146545
	3							3.400326	2.868400	2.323423	0.142489	0.145022	0.147023
		0°						2.083492	1.792991	1.481573	0.138639	0.142855	0.145804
90°	1	45°	0.1	0.1	0.5	2	0.1	2.067450	1.780738	1.471817	0.138573	0.142824	0.145788
		60°						2.056028	1.772039	1.464901	0.138526	0.142802	0.145777
		90°						2.028175	1.750919	1.448147	0.138409	0.142748	0.145749
			0	0				1.535564	1.298663	1.055482	0.086469	0.088686	0.090219
90°	1	45°	0	0.1	0.5	2	0.1	1.767773	1.502908	1.227527	0.107674	0.110736	0.112859
			0.1	0				1.800713	1.545699	1.273680	0.113068	0.116182	0.118350
			0.05	0.05				1.776898	1.517504	1.244663	0.110484	0.113566	0.115710
					0			2.028175	1.750919	1.448147	0.138409	0.142748	0.145749
90°	1	45°	0.1	0.1	0.5	2	0.1	2.067450	1.780738	1.471817	0.138573	0.142824	0.145788
					2			2.180895	1.868244	1.541863	0.139027	0.143039	0.145901
					4			2.323460	1.980802	1.633152	0.139558	0.143305	0.146045
						1		2.387201	2.055000	1.697909	0.137041	0.141996	0.145331
90°	1	45°	0.1	0.1	0.5	2	0.1	2.067450	1.780738	1.471817	0.138573	0.142824	0.145788
						5		1.849288	1.593467	1.317394	0.139659	0.143438	0.146139
						100		1.696680	1.462396	1.209288	0.140443	0.143895	0.146408
							0.3	2.115530	1.820144	1.504792	0.312419	0.334288	0.350711
							0.5	2.144058	1.845108	1.526718	0.417738	0.457174	0.488136
90°	1	45°	0.1	0.1	0.5	2	1	2.181950	1.880194	1.558953	0.560110	0.631956	0.691857
							5	2.237244	1.935622	1.613463	0.772897	0.912975	1.040890
							10	2.247189	1.946162	1.624354	0.811798	0.967084	1.111306

As noticed in Table 5, the inclined plate that is against the flow has the highest skin friction coefficient while for the Nusselt number, inclined plate that is along together with the flow has the highest Nusselt number.

Table 6 above shows the variation in skin friction coefficient at different dimensionless parameters for nanoparticles shape while Table 7 shows the variation of Nusselt number at different dimensionless parameters for shapes of nanoparticles. It is found that platelet nanoparticles shape has the highest skin friction and Nusselt number, followed by cylindrical shape, bricks shape and spherical shape. As spherical shape has the lowest skin friction coefficient and Nusselt number, it has been used to investigate the effect of parameters on velocity and temperature profile for all three conditions of inclined plate which are plate moving against the flow, $\varepsilon = -0.2$, static plate, $\varepsilon = 0$ and plate moving together with the flow, $\varepsilon = 0.2$.

Table 6
Variation in skin friction coefficient at different dimensionless parameters for Nanoparticles Shape Over an Inclined Plate

α	M	γ	ϕ_1	ϕ_2	λ_T	β_c	Bi_x	Skin Friction Coefficient			
								Spherical	Platelets	Cylindrical	Bricks
0°								0.836165	0.845148	0.842436	0.838750
45°	1	45°	0.1	0.1	0.5	2	0.1	1.385998	1.392028	1.390207	1.387733
70°								1.696291	1.701402	1.699860	1.697762
90°								1.780738	1.785646	1.784165	1.782151
	0							0.836165	0.845148	0.842436	0.838750
90°	1	45°	0.1	0.1	0.5	2	0.1	1.780738	1.785646	1.784165	1.782151
	2							2.386281	2.390103	2.388951	2.387382
	3							2.868400	2.871646	2.870669	2.869336
		0°						1.792991	1.799900	1.797815	1.794980
90°	1	45°	0.1	0.1	0.5	2	0.1	1.780738	1.785646	1.784165	1.782151
		60°						1.772039	1.775522	1.774471	1.773042
		90°						1.750919	1.750919	1.750919	1.750919
			0	0				1.298663	1.298663	1.298663	1.298663
90°	1	45°	0	0.1	0.5	2	0.1	1.502908	1.504543	1.504066	1.503395
			0.1	0				1.545699	1.548708	1.547741	1.546512
			0.05	0.05				1.517504	1.519928	1.519173	1.518180
					0			1.750919	1.750919	1.750919	1.750919
90°	1	45°	0.1	0.1	0.5	2	0.1	1.780738	1.785646	1.784165	1.782151
					2			1.868244	1.887249	1.881521	1.873722
					4			1.980802	2.017346	2.006347	1.991351
						1		2.055000	2.060501	2.058840	2.056583
90°	1	45°	0.1	0.1	0.5	2	0.1	1.780738	1.785646	1.784165	1.782151
						5		1.593467	1.597955	1.596601	1.594759
						100		1.462396	1.466581	1.465318	1.463601
							0.3	1.820144	1.829919	1.827002	1.822990
							0.5	1.845108	1.857077	1.853527	1.848615
90°	1	45°	0.1	0.1	0.5	2	1	1.880194	1.894148	1.890042	1.884315
							5	1.935622	1.950254	1.945984	1.939980
							10	1.946162	1.960595	1.956387	1.950464

Table 7
Variation in Nusselt Number at different dimensionless parameters for Nanoparticles Shape Over an Inclined Plate

α	M	γ	ϕ_1	ϕ_2	λ_T	β_c	Bi_x	Nusselt Number			
								Spherical	Platelets	Cylindrical	Bricks
0°								0.138897	0.180854	0.167640	0.150438
45°	1	45°	0.1	0.1	0.5	2	0.1	0.141563	0.184441	0.170936	0.153357
70°								0.142584	0.185829	0.172208	0.154478
90°								0.142824	0.186156	0.172507	0.154741
	0							0.138897	0.180854	0.167640	0.150438
90°	1	45°	0.1	0.1	0.5	2	0.1	0.142824	0.186156	0.172507	0.154741
	2							0.144209	0.188047	0.174237	0.156264
	3							0.145022	0.189159	0.175254	0.157158
		0°						0.142855	0.186206	0.172550	0.154777
90°	1	45°	0.1	0.1	0.5	2	0.1	0.142824	0.186156	0.172507	0.154741
		60°						0.142802	0.186119	0.172475	0.154716
		90°						0.142748	0.186031	0.172398	0.154653
			0	0				0.088686	0.088686	0.088686	0.088686
90°	1	45°	0	0.1	0.5	2	0.1	0.110736	0.124391	0.120330	0.114731
			0.1	0				0.116182	0.140647	0.132550	0.122576
			0.05	0.05				0.113566	0.133628	0.127214	0.119007
					0			0.142748	0.186031	0.172398	0.154653
90°	1	45°	0.1	0.1	0.5	2	0.1	0.142824	0.186156	0.172507	0.154741
					2			0.143039	0.186510	0.172814	0.154992
					4			0.143305	0.186942	0.173189	0.155299
						1		0.141996	0.185005	0.171460	0.153827
90°	1	45°	0.1	0.1	0.5	2	0.1	0.142824	0.186156	0.172507	0.154741
						5		0.143438	0.187007	0.173282	0.155419
						100		0.143895	0.187641	0.173859	0.155924
							0.3	0.334288	0.427346	0.398275	0.360111
							0.5	0.457174	0.577421	0.540033	0.490713
90°	1	45°	0.1	0.1	0.5	2	1	0.631956	0.784877	0.737614	0.674884
							5	0.912975	1.104492	1.045743	0.967172
							10	0.967084	1.164143	1.103759	1.022915

6. Conclusions

The effects of MHD and nanoparticles shape on boundary layer flow of Casson hybrid nanofluids over a moving inclined plate were explored in this study. A nonlinear PDE is converted to an ODE and numerically solved using the Keller Box method in Fortran software utilising the similarity approach. The convective boundary condition is considered as boundary conditions. The finding of this study can be concluded as follow:

(i) The velocity is increases and temperature is decreases due to the increasing of $\alpha, M, \gamma, \lambda_T, \beta_c$ and Bi_x
(ii) An increase in (ϕ_1, ϕ_2) depicts a decrement in the velocity profile but a rise in the temperature profiles.
(iii) When the value of Bi_x increases, the velocity and temperature profiles also increase.
(iv) The nanoparticles shape with the highest velocity and temperature profiles is platelet followed by cylindrical, bricks, and spherical.
(v) The skin friction and Nusselt number increase due to the increase in of $\alpha, M, \gamma, \lambda_T$, Bi_x but except for β_c.

(vi) The condition of plate with the highest skin friction is moving against the flow plate while the highest Nusselt number is the plate that is moving along the flow.

Acknowledgement
The authors extend their appreciation to Universiti Teknologi MARA Shah Alam for funding this work through "Geran Penyelidikan MyRA" under grant number 600-RMC 5/3/GPM (041/2022).

References

[1] Choi, S. US, and Jeffrey A. Eastman. *Enhancing thermal conductivity of fluids with nanoparticles*. No. ANL/MSD/CP-84938; CONF-951135-29. Argonne National Lab.(ANL), Argonne, IL (United States), 1995.
[2] Tiwari, Raj Kamal, and Manab Kumar Das. "Heat transfer augmentation in a two-sided lid-driven differentially heated square cavity utilizing nanofluids." *International Journal of Heat and Mass Transfer* 50, no. 9-10 (2007): 2002-2018. https://doi.org/10.1016/j.ijheatmasstransfer.2006.09.034
[3] Hayat, Tanzila, and S. Nadeem. "Heat transfer enhancement with Ag-CuO/water hybrid nanofluid." *Results in Physics* 7 (2017): 2317-2324. https://doi.org/10.1016/j.rinp.2017.06.034
[4] Sidik, Nor Azwadi Che, Idris M. Adamu, and Muhammad Mahmud Jamil. "Preparation methods and thermal performance of hybrid nanofluids." *Journal of Advanced Research in Applied Mechanics* 66, no. 1 (2020): 7-16. https://doi.org/10.37934/aram.66.1.716
[5] Manjunatha, S., B. Ammani Kuttan, S. Jayanthi, Ali Chamkha, and B. J. Gireesha. "Heat transfer enhancement in the boundary layer flow of hybrid nanofluids due to variable viscosity and natural convection." *Heliyon* 5, no. 4 (2019). https://doi.org/10.1016/j.heliyon.2019.e01469
[6] Akbar, Hanan Mohamad, Asan Suad Mohammed, and Sarah Burhan Ezzat. "Hybrid nanofluid to improve heat transfer and pressure drop through horizontal tube." *Materials Today: Proceedings* 42 (2021): 1885-1888. https://doi.org/10.1016/j.matpr.2020.12.227
[7] Bing, Kho Yap, Abid Hussanan, Muhammad Khairul Anuar Mohamed, Norhafizah Mohd Sarif, Zulkhibri Ismail, and Mohd Zuki Salleh. "Thermal radiation effect on MHD flow and heat transfer of Williamson nanofluids over a stretching sheet with Newtonian heating." In *AIP Conference Proceedings*, vol. 1830, no. 1. AIP Publishing, 2017. https://doi.org/10.1063/1.4980885
[8] Hussanan, Abid, Mohd Zuki Salleh, Ilyas Khan, and Sharidan Shafie. "Convection heat transfer in micropolar nanofluids with oxide nanoparticles in water, kerosene and engine oil." *Journal of Molecular Liquids* 229 (2017): 482-488. https://doi.org/10.1016/j.molliq.2016.12.040
[9] Aman, Sidra, Ilyas Khan, Zulkhibri Ismail, Mohd Zuki Salleh, Ali Saleh Alshomrani, and Metib Said Alghamdi. "Magnetic field effect on Poiseuille flow and heat transfer of carbon nanotubes along a vertical channel filled with Casson fluid." *AIP Advances* 7, no. 1 (2017). https://doi.org/10.1063/1.4975219
[10] Hussanan, Abid, Mohd Zuki Salleh, and Ilyas Khan. "Microstructure and inertial characteristics of a magnetite ferrofluid over a stretching/shrinking sheet using effective thermal conductivity model." *Journal of Molecular Liquids* 255 (2018): 64-75. https://doi.org/10.1016/j.molliq.2018.01.138
[11] Kho, Yap Bing, Abid Hussanan, Norhafizah Mohd Sarif, Zulkhibri Ismail, and Mohd Zuki Salleh. "Thermal radiation effects on MHD with flow heat and mass transfer in Casson nanofluid over a stretching sheet." In *MATEC Web of Conferences*, vol. 150, p. 06036. EDP Sciences, 2018. https://doi.org/10.1051/matecconf/201815006036
[12] Aman, Sidra, Ilyas Khan, Zulkhibri Ismail, Mohd Zuki Salleh, and Qasem M. Al-Mdallal. "Heat transfer enhancement in free convection flow of CNTs Maxwell nanofluids with four different types of molecular liquids." *Scientific Reports* 7, no. 1 (2017): 2445. https://doi.org/10.1038/s41598-017-01358-3
[13] Rawi, N. A., M. R. Ilias, Y. J. Lim, Z. M. Isa, and S. Shafie. "Unsteady mixed convection flow of Casson fluid past an inclined stretching sheet in the presence of nanoparticles." In *Journal of Physics: Conference Series*, vol. 890, no. 1, p. 012048. IOP Publishing, 2017. https://doi.org/10.1088/1742-6596/890/1/012048
[14] Mohamad, Ahmad Qushairi, Ilyas Khan, Lim Yeou Jiann, Arshad Khan, Mohd Rijal Ilias, and Sharidan Shafie. "Magnetohydrodynamic conjugate flow of casson fluid over a vertical plate embedded in a porous medium with arbitrary wall shear stress." *Journal of Nanofluids* 6, no. 1 (2017): 173-181. https://doi.org/10.1166/jon.2017.1294
[15] Bosli, Fazillah, Alia Syafiqa Suhaimi, Siti Shuhada Ishak, Mohd Rijal Ilias, Amirah Hazwani Abdul Rahim, and Anis Mardiana Ahmad. "Investigation of Nanoparticles Shape Effects on Aligned MHD Casson Nanofluid Flow and Heat Transfer with Convective Boundary Condition." *Journal of Advanced Research in Fluid Mechanics and Thermal Sciences* 91, no. 1 (2022): 155-171. https://doi.org/10.37934/arfmts.91.1.155171

[16] Krishna, M. Veera, N. Ameer Ahammad, and Ali J. Chamkha. "Radiative MHD flow of Casson hybrid nanofluid over an infinite exponentially accelerated vertical porous surface." *Case Studies in Thermal Engineering* 27 (2021): 101229. https://doi.org/10.1016/j.csite.2021.101229

[17] Aman, Sidra, Syazwani Mohd Zokri, Zulkhibri Ismail, Mohd Zuki Salleh, and Ilyas Khan. "Effect of MHD and porosity on exact solutions and flow of a hybrid Casson-nanofluid." *Journal of Advanced Research in Fluid Mechanics and Thermal Sciences* 44, no. 1 (2018): 131-139.

[18] Ishak, Siti Shuhada, Nurul Nurfatihah Mazlan, Mohd Rijal Ilias, Roselah Osman, Abdul Rahman Mohd Kasim, and Nurul Farahain Mohammad. "Radiation Effects on Inclined Magnetohydrodynamics Mixed Convection Boundary Layer Flow of Hybrid Nanofluids over a Moving and Static Wedge." *Journal of Advanced Research in Applied Sciences and Engineering Technology* 28, no. 3 (2022): 68-84. https://doi.org/10.37934/araset.28.3.6884

[19] Noranuar, Wan Nura'in Nabilah, Ahmad Qushairi Mohamad, Sharidan Shafie, Ilyas Khan, Lim Yeou Jiann, and Mohd Rijal Ilias. "Non-coaxial rotation flow of MHD Casson nanofluid carbon nanotubes past a moving disk with porosity effect." *Ain Shams Engineering Journal* 12, no. 4 (2021): 4099-4110. https://doi.org/10.1016/j.asej.2021.03.011

[20] Ilias, Mohd Rijal, Nur Sa'aidah Ismail, Nurul Hidayah AbRaji, Noraihan Afiqah Rawi, and Sharidan Shafie. "Unsteady aligned MHD boundary layer flow and heat transfer of a magnetic nanofluids past an inclined plate." *International Journal of Mechanical Engineering and Robotics Research* 9, no. 2 (2020): 197-206. https://doi.org/10.18178/ijmerr.9.2.197-206

[21] Ilias, Mohd Rijal, Noraihan Afiqah Rawi, N. H. A. Raji, and Sharidan Shafie. "Unsteady aligned MHD boundary layer flow and heat transfer of magnetic nanofluid past a vertical flate plate with leading edge accretion." *ARPN Journal of Engineering and Applied Sciences* 13, no. 1 (2018): 340-351.

[22] Mohamad, Ahmad Qushairi, Wan Nura'in Nabilah Noranuar, Zaiton Mat Isa, Sharidan Shafie, Abdul Rahman Mohd Kasim, Mohd Rijal Illias, and Lim Yeou Jiann. "Natural Convection Flow of Casson Fluid with Carbon Nanotubes Past an Accelerated Disk." In *International Conference on Mathematical Sciences and Statistics* 2022 (ICMSS 2022), pp. 484-497. Atlantis Press, 2022. https://doi.org/10.2991/978-94-6463-014-5_41

[23] Nayan, Asmahani, Nur Izzatie Farhana Ahmad Fauzan, Mohd Rijal Ilias, Shahida Farhan Zakaria, and Noor Hafizah Zainal Aznam. "Aligned Magnetohydrodynamics (MHD) Flow of Hybrid Nanofluid Over a Vertical Plate Through Porous Medium." *Journal of Advanced Research in Fluid Mechanics and Thermal Sciences* 92, no. 1 (2022): 51-64. https://doi.org/10.37934/arfmts.92.1.5164

[24] Ismail, Nur Suhaida Aznidar, Ahmad Sukri Abd Aziz, Mohd Rijal Ilias, and Siti Khuzaimah Soid. "Mhd boundary layer flow in double stratification medium." In *Journal of Physics: Conference Series*, vol. 1770, no. 1, p. 012045. IOP Publishing, 2021. https://doi.org/10.1088/1742-6596/1770/1/012045

[25] Khashi'ie, Najiyah Safwa, Norihan Md Arifin, Ezad Hafidz Hafidzuddin, Nadihah Wahi, and Mohd Rijal Ilias. "Magnetohydrodynamics (MHD) flow and heat transfer of a doubly stratified nanofluid using Cattaneo-Christov model." *Universal Journal of Mechanical Engineering* 7, no. 4 (2019): 206-214. https://doi.org/10.13189/ujme.2019.070409

[26] Rosaidi, Nor Alifah, Nurul Hidayah Ab Raji, Siti Nur Hidayatul Ashikin Ibrahim, and Mohd Rijal Ilias. "Aligned magnetohydrodynamics free convection flow of magnetic nanofluid over a moving vertical plate with convective boundary condition." *Journal of Advanced Research in Fluid Mechanics and Thermal Sciences* 93, no. 2 (2022): 37-49. https://doi.org/10.37934/arfmts.93.2.3749

[27] Ishak, Siti Shuhada, Nurin Nisa Mohd Noor Azhar, Nurul Syafiqah Nazli, Mohd Rijal Ilias, Roselah Osman, Zubaidah Sadikin, Abdul Rahman Mohd Kasim, and Nurul Farahain Mohammad. "Carbon Nanotubes Flow on Mixed Convection of Aligned Magnetohydrodynamics over a Static/Moving Wedge with Convective Boundary Conditions." *CFD Letters* 15, no. 7 (2023): 74-91. https://doi.org/10.37934/cfdl.15.7.7491

[28] Ab Raji, Nurul Hidayah, Nurul Samiha Mohd Shahabudin, Noorehan Awang, Mohd Rijal Ilias, and Siti Shuhada Ishak. "Aligned Magnetohydrodynamics Mixed Convection on Various Base Fluids with Carbon Nanotubes over an Inclined Plate." *CFD Letters* 15, no. 6 (2023): 12-25. https://doi.org/10.37934/cfdl.15.6.1225

[29] Bosli, Fazillah, Mohd Rijal Ilias, Noor Hafizah Zainal Aznam, Siti Shuhada Ishak, Shahida Farhan Zakaria, and Amirah Hazwani Abdul Rahim. "Aligned magnetohydrodynamic effect on magnetic nanoparticle with different base fluids past a moving inclined plate." *International Journal of Advanced and Applied Sciences* 10, no. 3 (2023): 96-107. https://doi.org/10.21833/ijaas.2023.03.013

[30] Rashid, Umair, and Adnan Ibrahim. "Impacts of nanoparticle shape on Al_2O_3-water nanofluid flow and heat transfer over a non-linear radically stretching sheet." *Advances in Nanoparticles* 9, no. 01 (2020): 23-39. https://doi.org/10.4236/anp.2020.91002

[31] Anwar, Talha, Poom Kumam, and Phatiphat Thounthong. "A comparative fractional study to evaluate thermal performance of NaAlg-MoS_2-Co hybrid nanofluid subject to shape factor and dual ramped conditions." *Alexandria Engineering Journal* 61, no. 3 (2022): 2166-2187. https://doi.org/10.1016/j.aej.2021.06.085

[32] Akbar, Noreen Sher, and Adil Wahid Butt. "Ferromagnetic effects for peristaltic flow of Cu-water nanofluid for different shapes of nanosize particles." *Applied Nanoscience* 6 (2016): 379-385. https://doi.org/10.1007/s13204-015-0430-x
[33] Jamshed, Wasim, Nor Ain Azeany Mohd Nasir, Ameni Brahmia, Kottakkaran Sooppy Nisar, and Mohamed R. Eid. "Entropy analysis of radiative [$MgZn_6Zr$-Cu/EO] Casson hybrid nanoliquid with variant thermal conductivity along a stretching surface: Implementing Keller box method." *Proceedings of the Institution of Mechanical Engineers, Part C: Journal of Mechanical Engineering Science* 236, no. 12 (2022): 6501-6520. https://doi.org/10.1177/09544062211065696
[34] Zukri, Norsyasya Zahirah Mohd, Mohd Rijal Ilias, Siti Shuhada Ishak, Roselah Osman, Nur Asiah Mohd Makhatar, and Mohd Nashriq Abd Rahman. "Magnetohydrodynamic Effect in Mixed Convection Casson Hybrid Nanofluids Flow and Heat Transfer over a Moving Vertical Plate." *CFD Letters* 15, no. 7 (2023): 92-111. https://doi.org/10.37934/cfdl.15.7.92111
[35] Casson, N. "A flow equation for the pigment oil suspension of the printing ink type." *Rheology of Disperse Systems* (1959): 84-104.
[36] Na, Tsung Y., and Arthur G. Hansen. "Similarity analysis of differential equations by Lie group." *Journal of the Franklin Institute* 292, no. 6 (1971): 471-489. https://doi.org/10.1016/0016-0032(71)90167-0
[37] Cebeci, Tuncer, and Peter Bradshaw. *Physical and computational aspects of convective heat transfer*. Springer Science & Business Media, 2012.
[38] Bataller, Rafael Cortell. "Radiation effects for the Blasius and Sakiadis flows with a convective surface boundary condition." *Applied Mathematics and Computation* 206, no. 2 (2008): 832-840. https://doi.org/10.1016/j.amc.2008.10.001
[39] Aziz, Abdul. "A similarity solution for laminar thermal boundary layer over a flat plate with a convective surface boundary condition." *Communications in Nonlinear Science and Numerical Simulation* 14, no. 4 (2009): 1064-1068. https://doi.org/10.1016/j.cnsns.2008.05.003
[40] Ishak, Anuar, Nor Azizah Yacob, and Norfifah Bachok. "Radiation effects on the thermal boundary layer flow over a moving plate with convective boundary condition." *Meccanica* 46 (2011): 795-801. https://doi.org/10.1007/s11012-010-9338-4
[41] Ramesh, G. K., A. J. Chamkha, and B. J. Gireesha. "Boundary layer flow past an inclined stationary/moving flat plate with convective boundary condition." *Afrika Matematika* 27 (2016): 87-95. https://doi.org/10.1007/s13370-015-0323-x